Cosmological perturbations in a genuinely phantom dark energy Universe

Imanol Albarran, Mariam Bouhmadi-López and João Morais

Centro de Matemática e Aplicações. Universidade da Beira Interior (Portugal).

work in progress

VARCOSMOFUN'16

September 12, 2016

Universidade da Beira Interior

Outline

1 Introduction

- Small deviations in the temperature of CMB $\Rightarrow$ Isotropy.
- Copernican Principle $\Rightarrow$ Homogeneity at large scales.

FLRW space time metric:

$$g_{\mu\nu} = -dt^2 + a(t)^2 \left[\left(\frac{1}{1 - kr^2} \right) dr^2 + r^2 d\theta^2 + r^2 \sin^2(\theta) d\varphi^2 \right],$$

where $a(t)$ is the scale factor and $k = -1, 0, 1$.

- Late-time acceleration $\Rightarrow$ Existence of dark energy.
- Dark energy density can be described as:

$$\rho_d = \rho_{d0} a^{-3(1+w_d)}, \quad \text{where} \quad w_d \approx -1,$$

- Best fit given by ΛCDM model, where $w_d = -1$.

∗ what happens if the cosmological constant is not quite constant?

- The tiniest deviation in w_d can induce a range of different future events.

Background models

- Each model induce an unique abrupt event:

∗ Model (i) $\Rightarrow$ Big Rip (BR)
∗ Model (ii) $\Rightarrow$ Little Rip (LR)
∗ Model (iii) $\Rightarrow$ Little Sibling of the Big Rip (LSBR)

Event	Divergence	$p_d = p_d(\rho)$
BR	$a, \lvert H \rvert, \lvert \dot{H} \rvert \to \infty, \quad t < \infty$	$p_d = w_d \rho_d,$
LR	$t, a, \lvert H \rvert, \lvert \dot{H} \rvert \to \infty$	$p_d = -\rho - B\rho_d^{\frac{1}{2}}$
LSBR	$t, a, \lvert H \rvert \to \infty, \quad \lvert \dot{H} \rvert < \infty$	$p_d = -\rho_d - A$

Where $w_d < -1$ and the parameters A and B are positive.

Perturbed equations-1

- We choose the Newtonian gauge. For FLRW universe the perturbed line element is

$$ds^2 = a^2\left[-\left(1+2\Psi\right)d\eta^2 + \left(1-2\Phi\right)\delta_{ij}dx^i dx^j\right],$$

where η is the comoving time and Ψ and Φ the Bandeen potentials.
- Christoffel Symbols $\Rightarrow$ Ricci scalar and curvature $\Rightarrow$ Perturbed Einstein equation.

$$\delta G^{\mu}_{\ \nu} = 8\pi G \delta T^{\mu}_{\ \nu},$$

- The individual components can be written as

$$-\nabla^2\Psi + 3\mathcal{H}\left(\Phi\mathcal{H} + \Psi'\right) = -4\pi G a^2 \delta T^{0}_{\ 0},$$

$$\left[\mathcal{H}\Phi + \Psi'\right]_{,i} = -4\pi G a^2 \delta T^{0}_{\ i},$$

$$3\Psi'' + \frac{2}{3}\nabla^2\left(\Phi - \Psi\right) + 2\mathcal{H}\left(\Phi' + 2\Psi'\right) + 2\Phi\left(2\mathcal{H}' + \mathcal{H}^2\right)\Phi = \frac{4}{3}\pi G a^2 \delta T^{i}_{\ i},$$

$$\left[\Phi - \Psi\right]_{,ij} = 8\pi G a^2 \delta T^{i}_{\ j}. \qquad (i \neq j)$$

Perturbed equations-2

- $\delta T^{\mu}_{\ \nu}$ is the sum of the perturbed energy momentum tensor of different fluids i.e. $\delta T^{\mu}_{\ \nu} = \delta T^{\mu}_{r\,\nu} + \delta T^{\mu}_{m\,\nu} + \delta T^{\mu}_{d\,\nu}$. For a fluid called A;

$$\begin{aligned}
\delta T^{0}_{A\,0} &= -\,\delta\rho_A,\\
\delta T^{i}_{A\,0} &= -\,(p+\rho)\,\partial^i v_A,\\
\delta T^{0}_{A\,i} &= (p+\rho)\,\partial_i v_A,\\
\delta T^{i}_{A\,j} &= \delta p_A\ \delta^i_j + \Pi^i_{A\,j}.
\end{aligned}$$

- No anisotropic stress tensor; $\Pi^i_{A\,j} = 0$ implies $\Psi = \Phi$, then, we have:

$$\begin{aligned}
\nabla^2\Psi + 3\mathcal{H}\left(\mathcal{H}\Psi - \Psi'\right) &= 4\pi G a^2 \delta\rho,\\
\nabla^2\left(\mathcal{H}\Psi + \Psi'\right) &= -4\pi G a^2\left(\rho + p\right)\nabla^2 v,\\
\Psi'' + 3\mathcal{H}\Psi' + \Psi\left(2\mathcal{H}' + \mathcal{H}^2\right) &= 4\pi G a^2 \delta p,
\end{aligned}$$

Perturbed equations-3

- The pressure can be decompose in the following way

$$\delta p_A = c_{sA}^2 \delta\rho_A - 3\mathcal{H}\left(1 + w_A\right)\left(c_{sA}^2 - c_{aA}^2\right)\rho_A v_A,$$

where $c_{sA}^2 = \frac{\delta p_A}{\delta \rho_A}\Big|_{r.f}$ and $c_{aA}^2 = \frac{p_A'}{\rho_A'}$, are respectively the effective speed of sound in the rest frame and the adiabatic speed of sound.

- The fluids are conserved separately, that means

$$\nabla_\mu \delta T^{\mu}_{A\,\nu} + \delta\Gamma^{\mu}_{\mu\alpha} T^{\alpha}_{A\,\nu} - \delta\Gamma^{\alpha}_{\mu\nu} T^{\mu}_{A\,\alpha} = 0,$$

leading to the equations

$$\delta_A' = \left(1 + w_A\right)\left\{\left[k^2 + 9\mathcal{H}\left(c_{sA}^2 - c_{aA}^2\right)\right] v_A + 3\Psi'\right\} + 3\left(w_A - c_{sA}^2\right)\delta_A,$$

$$v_A' = \left(3c_{sA}^2 - 1\right)\mathcal{H} v_A - \frac{c_{sA}^2}{1 + w_A}\delta_A - \Psi.$$

Perturbed equations-4

- Decomposition into Fourier components, therefore, for practical purposes, we make the substitution $\nabla^2 \rightarrow -k^2$
- We apply the change of variable $x \equiv \ln(a)$, therefore, $\{\}' = \{\}_x \mathcal{H}$
- The set of dynamical equations for each component can be written as

∗ Radiation component

$$\delta_{rx} = \frac{4}{3}\left(\frac{k^2}{\mathcal{H}} v_r + 3\Psi_x\right) \quad , \quad v_{rx} = -\frac{1}{\mathcal{H}}\left(\frac{1}{4}\delta_r + \Psi\right)$$

∗ Matter component

$$\delta_{mx} = \frac{k^2}{\mathcal{H}} v_r + 3\Psi_x \quad , \quad v_{mx} = -v_m - \frac{\Psi}{\mathcal{H}}$$

Perturbed equations-5

∗ DE component

$$\delta_{dx} = (1+w_d)\left\{\left[\frac{k^2}{\mathcal{H}} + 9\mathcal{H}\left(1-c_{ad}^2\right)\right] v_d + 3\Psi_x\right\} + 3\left(w_d - 1\right)\delta_d,$$
$$v_{dx} = -\frac{1}{\mathcal{H}}\left[\frac{1}{1+w_d}\delta_d + \Psi\right] + 2v_d.$$

- The metric potential satisfies:

$$\Psi_x + \Psi\left(1 + \frac{k^2}{3\mathcal{H}^2}\right) = -\frac{1}{2}\delta,$$
$$\Psi_x + \Psi = -\frac{3}{2}\mathcal{H}v\left(1+w\right),$$
$$\Psi_{xx} + \left[3 - \frac{1}{2}\left(1+3w\right)\right]\Psi_x - 3w\Psi = \frac{3}{2}\frac{\delta p}{\rho}.$$

DE as a phantom scalar field

• Matter and radiation described as a barotropic fluid where $c_{sA}^2 = c_{aA}^2$.
• For fluids with a negative EoS there might be some problems since $c_{aA}^2 < 0$, leading to undesirable instabilities.
• We follow the strategy applied in (R. Bean '03, J. Väliviita '08) which consists into map the dark energy to a scalar field, φ, where the variations of energy density and pressure are

$$\delta\rho_\varphi = -\dot{\varphi}\left(\delta\dot{\varphi} + \dot{\varphi}\Psi\right) + \frac{\delta V}{\partial\varphi}\delta\varphi,$$
$$\delta p_\varphi = -\dot{\varphi}\left(\delta\dot{\varphi} + \dot{\varphi}\Psi\right) - \frac{\delta V}{\partial\varphi}\delta\varphi.$$

• The rest frame is defined by constant φ surfaces i.e. $\delta\varphi = 0$. Therefore, $\delta\rho_\varphi = \delta p_\varphi$ and we set $c_{sA}^2 = 1$ (A. V. Astashenok and S. D. Odintsov '12).
• This mapping of the DE fluid to a phantom scalar field removes any instabilities in the energy density of the scalar perturbations of DE.

Initial conditions-1

- We impose;

$*$ At an initial moment, $x_* \approx -14$, the Universe was completely dominated by radiation i.e. $p = (1/3)\,\rho$

$*$ At such moment all the relevant comoving wave-numbers of the modes are small when compared with the comoving Hubble parameter, i.e $k \ll \mathcal{H}$.

$*$ Combining the above approximations with the equation set it is found that $\Psi_{xx} + 3\Psi_x \approx 0$. Therefore, the dominant solution is constant.

$*$ Assuming initial adiabatic conditions, we can relate the initial values of the individual fluid perturbation variables to the total perturbation.

$$\frac{3}{4}\delta_r\left(x_*\right) = \delta_m\left(x_*\right) = \frac{\delta_d\left(x_*\right)}{1 + w_d\left(x_*\right)} = \frac{3}{4}\delta\left(x_*\right),$$

$$v_r\left(x_*\right) = v_m\left(x_*\right) = v_d\left(x_*\right) \approx \frac{\delta\left(x_*\right)}{4\mathcal{H}(x_*)}.$$

Initial conditions-2

- Making use of the linearity properties, we can first compute the evolution of the perturbation quantities using the initial conditions for $\Psi(x_*) = 1$.
- Then, we multiply all the solutions obtained by the physical value of $\delta(x_*)$, which we will take from the Planck observational fit to single field inflation.

$$\delta(x_*) = \frac{8}{3}\pi\sqrt{2A_s}\left(\frac{k}{k_*}\right)^{\frac{n_s-1}{2}} k^{-\frac{3}{2}},$$

where A_s and n_s are the amplitude and spectral index of the primordial power spectrum corresponding to the selected pivot scale k_*. We use the values $k_* = 0.05\ \mathrm{Mpc}^{-1}$, $A_s = 2.143 \cdot 10^{-9}$, and $n_s = 0.9681$ in accordance with the latest observational data (Planck '15).

Matter power spectrum and growth rate

• With the aim to compare the theoretical predictions with the observational data, we will compute the matter power spectrum and the growth rate for each model.

∗ Matter power spectrum

Matter power spectrum is usually calculated in the comoving gauge rather than in the Newtonian gauge.

$$P_{\hat{\delta}_m} = \left|\delta_m^{(com)}\right|^2 = \left|\delta_m - 3\mathcal{H}v_m\right|^2 .$$

We will compare the results with the ΛCDM model.

∗ Growth rate

$$f \equiv \frac{d\left(\ln \delta_m\right)}{d\left(\ln a\right)}.$$

We compare our results with SSDS III data (S. Satpathy '16).

Results-1

• For each of these models, the evolution of the matter perturbations δ_m, v_m, δ_r, v_r, δ_d, and v_d was obtained by numerically integrating the previous set of equations.

• The integration was performed since an initial moment deep inside the radiation epoch ($z \sim 10^6$), till a point in the distant future ($z \sim -0.99$).

• For each model this integration was repeated for several different modes with wave-numbers ranging from a $k_{\text{min}} \sim 3.3 \cdot 10^{-4}\text{h Mpc}^{-1}$, to a $k_{\text{max}} \sim 3.0 \cdot 10^{-1}\text{h Mpc}^{-1}$.

$*$ For the following examples we have used 6 different wave-numbers classified as

Large: $k = 6.80 \cdot 10^{-2}\mathrm{h\ Mpc}^{-1}$ and $k = 0.30\ \mathrm{h\ Mpc}^{-1}$.

Medium: $k = 3.50 \cdot 10^{-3}\mathrm{h\ Mpc}^{-1}$ and $k = 1.54 \cdot 10^{-2}\mathrm{h\ Mpc}^{-1}$

Small: $k = 3.33 \cdot 10^{-4}\mathrm{h\ Mpc}^{-1}$ and $k = 7.93 \cdot 10^{-4}\mathrm{h\ Mpc}^{-1}$,

Results-2 (Matter perturbations)

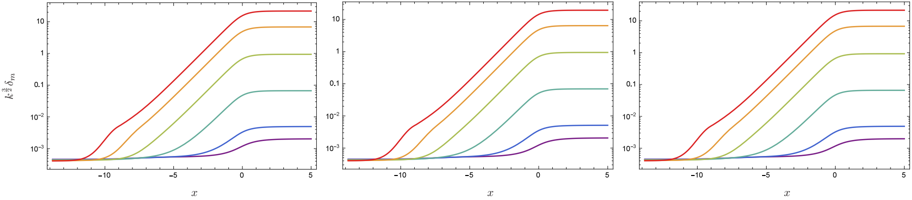

(i) (ii) (iii)

- The matter perturbations for the different models present an almost identical behaviour.
- During the radiation dominated epoch, each individual mode remains constant until it enters the Hubble horizon.
- Then, the gravitational collapse leads to the growth of δ_m, which becomes exponential in x during the matter era.
- Once DE starts to become dominant, the growth of the matter perturbations slows down and δ_m converges to a constant value in the asymptotic future.

Results-3 (DE perturbations)

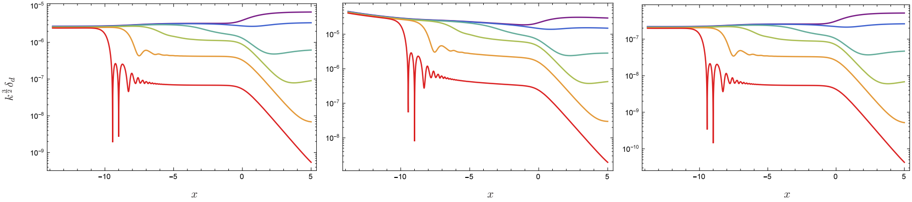

(i) (ii) (iii)

- The modes with large wave-numbers enter the horizon at earlier times and oscillate in the radiation dominated era. During the matter dominated era reach a plateau and decay rapidly when DE takes over.
- The modes with medium wave-numbers enter the horizon in the matter epoch with an almost constant value. When DE dominates the amplitude decay vanishing in the far future.
- For the smallest wave-numbers there is no decay and it can be seen how the modes are slight amplified reaching a plateau at late times.
- The imposition of initial conditions induce a similar behaviour, where the difference lays in the magnitude depending on the model.

Results-4 (Gravitational potential)

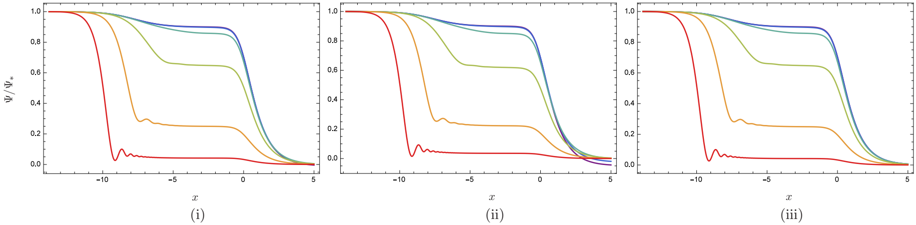

- The modes with large wave-numbers enter the horizon in the radiation epoch and decay rapidly, then, remain constant on the matter epoch and decay rapidly when DE takes over.
- The modes with medium wave-numbers, enter the horizon during the matter domination era and decay reaching a constant value till the present time. Finally, in the DE domination epoch decay and vanish.
- The modes with small wave-numbers enter the horizon well inside the matter era and reaches a plateau, vanishing in the far future.
- As theoretically expected, for the limit $k \to 0$ the modes are suppressed by a factor of 0.9 during matter domination.

Results-5 (Matter power spectrum)

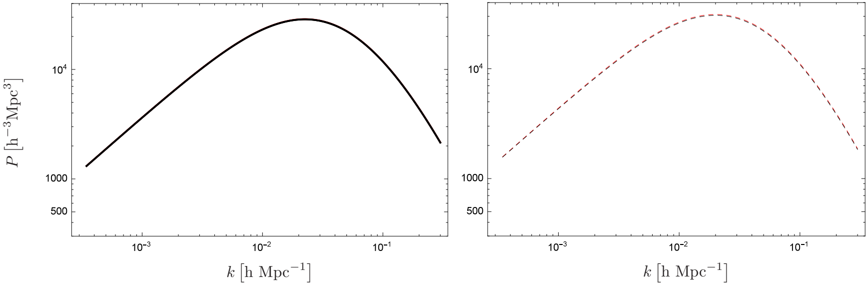

- In order to compare the models with ΛCDM it s necessary to impose the same model parameters. We have two set of constants according with the different fits.

∗ In the left panel: Model (i) and (iii) together to ΛCDM model.

∗ In the right panel: Model (ii) together to ΛCDM model.

- The models (i) and (iii) are indistinguishable from ΛCDM.
- The model (ii) present a very slight deviation from ΛCDM.

Results-5 (relative deviation respect to ΛCDM)

- In order to draw a comparison between the models, we compute the relative deviation with the corresponding ΛCDM model in each case.

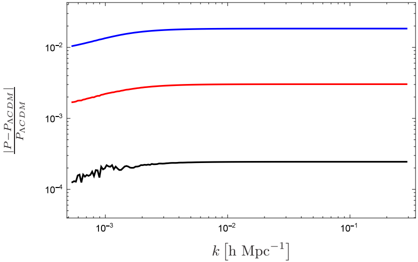

∗ Blue curve corresponds to model (i) → induce a BR
∗ Red curve corresponds to model (ii) → induce a LR
∗ Black curve corresponds to model (iii) → induce a LSBR

- For large values of the wave-number k, all models present a constant difference respect to ΛCDM model while for small values of k the deviation is smaller. In all cases, the relative deviation is less than a 0.02.

Results-6 (Growth rate)

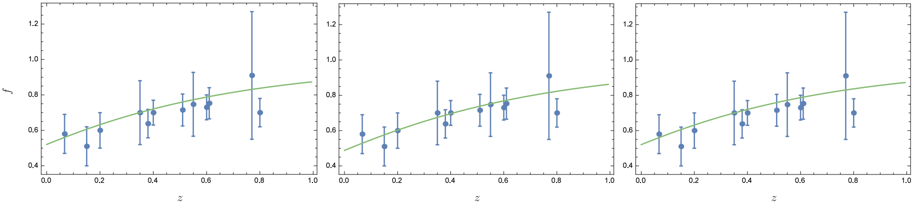

(i) (ii) (iii)

- We compute the growth rate of the different models and we compare it with the latest SDSS III data.
- We quantify the deviation from the observational data by computing χ^2 (A. Balcerzak and T. Denkiewicz '12).

$$\chi^2 = \sum_i \frac{\left[f_{obs}\left(z_i\right) - f_{th}\left(z_i\right)\right]^2}{\sigma_i^2},$$

- We obtain: $\chi^2_{(i)} = 5.90$, $\chi^2_{(ii)} = 3.74$, and $\chi^2_{(iii)} = 5.75$.

Conclusions

- In this work, we study the classical perturbations of three different models of DE that have a phantom character and induce, respectively, a BR, LR and LSBR.
- Asides from the DM and DE perturbations we compute the matter power spectrum and growth rate, comparing results with the latests SDSS III data.
- Although the ΛCDM model gives the best observational fit there is no strong evidence to disregard the models presented in this talk.
- At late time, the value of the EoS for each model are very similar, in consequence, the predictions given by each model are nearly identical which make us difficult to identify the footprint of each one.

Acknowledgements

This work was supported by the fellowship "Bolsas de Investigação Faculdade de Ciências (UBI)-Santander Totta" (Portugal).

Thank you for your attention!